

Arabidopsis thaliana RGXT1 and RGXT2 Encode Golgi-Localized (1,3)- α -D-Xylosyltransferases Involved in the Synthesis of Pectic Rhamnogalacturonan-II

Jack Egelund,^a Bent Larsen Petersen,^a Mohammed Saddik Motawia,^b Iben Damager,^a Ahmed Faik,^{c,1} Carl Erik Olsen,^d Tadashi Ishii,^e Henrik Clausen,^f Peter Ulvskov,^a and Naomi Geshi^{a,2,3}

^aBiotechnology Group, Danish Institute of Agricultural Sciences and Center for Molecular Plant Physiology, DK-1871 Frederiksberg C, Denmark

^bPlant Biochemistry Laboratory, Department of Plant Biology and Center for Molecular Plant Physiology, Royal Veterinary and Agricultural University, DK-1871 Frederiksberg C, Denmark

^cPlant Research Laboratory, Michigan State University, East Lansing, Michigan 48824

^dDepartment of Natural Sciences and Center for Molecular Plant Physiology, Royal Veterinary and Agricultural University, DK-1871 Frederiksberg C, Denmark

^eForestry and Forest Research Institute, Tsukuba Norin Kenkyu Danchi-nai, Ibaraki 305-8687, Japan

^fDepartment of Medical Biochemistry and Genetics, University of Copenhagen, DK-2200 Copenhagen N, Denmark

Two homologous plant-specific *Arabidopsis thaliana* genes, *RGXT1* and *RGXT2*, belong to a new family of glycosyltransferases (CAZy GT-family-77) and encode cell wall (1,3)- α -D-xylosyltransferases. The deduced amino acid sequences contain single transmembrane domains near the N terminus, indicative of a type II membrane protein structure. Soluble secreted forms of the corresponding proteins expressed in insect cells showed xylosyltransferase activity, transferring D-xylose from UDP- α -D-xylose to L-fucose. The disaccharide product was hydrolyzed by α -xylosidase, whereas no reaction was catalyzed by β -xylosidase. Furthermore, the regio- and stereochemistry of the methyl xylosyl-fucoside was determined by nuclear magnetic resonance to be an α -(1,3) linkage, demonstrating the isolated glycosyltransferases to be (1,3)- α -D-xylosyltransferases. This particular linkage is only known in rhamnogalacturonan-II, a complex polysaccharide essential to vascular plants, and is conserved across higher plant families. Rhamnogalacturonan-II isolated from both *RGXT1* and *RGXT2* T-DNA insertional mutants functioned as specific acceptor molecules in the xylosyltransferase assay. Expression of *RGXT1*- and *RGXT2*-enhanced green fluorescent protein constructs in *Arabidopsis* revealed that both fusion proteins were targeted to a Brefeldin A-sensitive compartment and also colocalized with the Golgi marker dye BODIPY TR ceramide, consistent with targeting to the Golgi apparatus. Taken together, these results suggest that *RGXT1* and *RGXT2* encode Golgi-localized (1,3)- α -D-xylosyltransferases involved in the biosynthesis of pectic rhamnogalacturonan-II.

INTRODUCTION

The polymers of the plant cell wall (CW) collectively determine its mechanical properties at the cell and tissue level, and the development and refinement of the CW have probably played a critical role for the colonization of dry land and the subsequent success of vascular plants. While vascular plants share a cellulose-xyloglucan load bearing structure with, for example, the bryophytes, differences among taxa in other CW polysaccharides appear to correlate well with their evolutionary relation-

ships (Popper and Fry, 2003). One of the CW features that distinguishes vascular plants is the pectic polymer rhamnogalacturonan-II (RG-II), which endows the wall with mechanical strength and probably was critical for the development of higher plants. RG-II consists of a linear polysaccharide of (1,4)- α -linked D-galacturonic acid (D-GalA) residues to which side chains (A–D and possibly also the fifth chain, E) are attached to positions O-2 or O-3 of the backbone of D-GalA residues (O'Neill et al., 1990; Vidal et al., 2000; O'Neill and York, 2003; Rodríguez-Carvajal et al., 2003). RG-II consists of 12 different glycosyl residues, including the rare sugars, D-apiose (D-Api), L-aceric acid (3-C-carboxy-5-deoxy-L-xylose), 2-O-methyl L-fucose, 2-O-methyl D-xylose (2-O-Me-D-Xyl), L-galactose, 3-deoxy-D-lyxo-heptulosaric acid, and 3-deoxy-D-manno-oct-2-ulonic acid, linked together by no less than 22 different glycosidic linkages. The structure of RG-II is highly conserved in all vascular plants examined to date, while lower land plants appear to have a 100-fold lower content of a polysaccharide that shares at least some of the rare monosaccharides with RG-II (Matsunaga et al., 2004).

RG-II exists predominantly as a dimer in planta (Ishii and Matsunaga, 1996; Kobayashi et al., 1996; O'Neill et al., 1996)

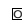
¹ Current address: Department of Environmental and Plant Biology, Ohio University, Athens, OH 45701.

² Current address: Department of Plant Biology, Royal Veterinary and Agricultural University, 1871 Frederiksberg C, Denmark.

³ To whom correspondence should be addressed. E-mail nge@kvl.dk; fax 45-35283333.

The author responsible for distribution of materials integral to the findings presented in this article in accordance with the policy described in the Instructions for Authors (www.plantcell.org) is: Naomi Geshi (nge@kvl.dk).

 Online version contains Web-only data.

 Open Access articles can be viewed online without a subscription. www.plantcell.org/cgi/doi/10.1105/tpc.105.036566

mediated by a borate diester bond formed with two apiosyl residues in the A-chain of each of the two RG-II monomers (O'Neill et al., 1996; Ishii et al., 1999). It is uncertain whether boron is required by lower land plants (Matsunaga et al., 2004), but it is an essential micronutrient for vascular plants and has been shown to be indispensable for RG-II dimerization, which in turn affects CW porosity (Fleischer et al., 1999; Ishii et al., 2001; Ryden et al., 2003). Two mutants, the *Arabidopsis thaliana mur1* (O'Neill et al., 2001) and the haploid *Nicotiana plumbaginifolia nolac H18* mutant (Iwai et al., 2002), have an altered RG-II sugar composition and are impaired in their ability to form RG-II dimers. Ahn et al. (2006) used virus-induced gene silencing to deplete the pool of UDP- α -D-Api and hence compromise both RG-II A- and B-chain synthesis. Like *nolac H18*, the CW phenotype was severe, and cell adhesion was clearly affected. Supply of borate to *mur1* and complementation of *nolac H18* with the corresponding wild-type allele (*N. plumbaginifolia GUT1*) restored their ability to form RG-II dimers. The ability to form boron-mediated RG-II dimers thus seems to be crucial for normal growth and development in higher plants.

Although the structure and functional significance of pectin is relatively well understood (reviewed in Ridley et al., 2001; Willats et al., 2001), little is known about the enzymatic apparatus involved in its biosynthesis. Different epitopes present in pectin have been detected in various compartments of the Golgi apparatus (Staehelein and Moore, 1995; Willats et al., 2001), and enzymes synthesizing pectin have been detected in Golgi-derived vesicles (Goubet and Mohnen, 1999; Sterling et al., 2001; Geshi et al., 2004), indicating that pectin is indeed synthesized in the Golgi apparatus. Glycosyltransferases (GTs) located in the Golgi apparatus typically have a type II membrane protein structure consisting of a single N-terminal transmembrane domain (TMD), followed by a stem-like region of variable length and the C-terminal catalytic domain facing the lumen of the Golgi apparatus (Breton et al., 2001). A processive mannan synthase with multiple membrane-spanning domains has been identified in the Golgi apparatus of guar (Dhugga et al., 2004), raising the possibility that enzymes other than type II membrane GTs may be involved in pectin biosynthesis. It is estimated that at least 53 different activities are required to form the glycosidic linkages present in pectin (Ridley et al., 2001). Biochemical and reverse genetic approaches have been used to identify genes that encode the GTs responsible for pectin biosynthesis. A dwarfed *Arabidopsis* mutant, *quasimodo1 (qua1)*, has been shown to have an \sim 25% reduction in D-GalA content and is presumably disrupted in a gene encoding a galacturonosyltransferase (Bouton et al., 2002), which is consistent with the recent finding that galacturonosyltransferase activity was reduced 23 to 33% in detergent-solubilized membrane fractions from *qua1* (Orfila et al., 2005). In addition, characterization of a transposon-tagged *Arabidopsis* homologue of *QUA1* showed reduced levels of rhamnogalacturonan-I (RG-I) branching and alterations in the abundance of some xyloglucan linkages (Lao et al., 2003). A galacturonosyltransferase solubilized from tobacco (*Nicotiana tabacum*) membranes elongates a homogalacturonan acceptor (Doong et al., 1995), and an *Arabidopsis* galacturonosyltransferase (*GAUT1*) involved in homogalacturonan biosynthesis has recently been functionally characterized by heterologous ex-

pression of the corresponding protein (Sterling et al., 2006). In addition, Harholt et al. (2006) recently identified a putative arabinosyltransferase (*ARAD1*) in *Arabidopsis*, which has been proposed to be involved in RG-I side chain biosynthesis, based on a 30% reduction of α -1,5-linked L-Araf in the corresponding T-DNA insertion mutant.

The Np *GUT1* gene shows discernible sequence similarity to animal glucuronosyltransferases, and the absence of glucuronic acid (D-GlcA) in RG-II of the *nolac H18* mutant have made the corresponding wild-type allele (Np *GUT1*) a good candidate for a glucuronosyltransferase-encoding gene with a role in RG-II biosynthesis (Iwai et al., 2002). *GAUT1* is so far the only GT involved in pectin biosynthesis for which enzymatic activity has been demonstrated by heterologous expression of the protein, and notably, the enzymatic activities of the *QUA1*- (also referred to as *GAUT8*) and the Np *GUT1* gene products remain to be demonstrated.

In this article, we characterize two homologous *Arabidopsis* GT-encoding genes that show no similarity to genes from other phyla, and we demonstrate that both genes encode (1,3)- α -D-xylosyltransferases and propose that they are involved in the biosynthesis of pectic RG-II.

RESULTS

Gene Identification and Deduced Protein Structure

The uniqueness and complexity of plant CW polysaccharide structures have made identification of CW GTs by simple homology approaches impracticable. In addition, the very limited number of donor and especially acceptor substrates has further hampered the identification of novel plant CW GTs. As a significant proportion of *Arabidopsis* GTs probably remains to be classified, we developed a bioinformatic filtering strategy aimed at identifying unclassified CW GTs in *Arabidopsis* (Egelund et al., 2004). As a result, 27 putative GTs were identified, and two of these gave rise to a new family in CAZy (GT-family-77; Coutinho et al., 2003a; <http://afmb.cnrs-mrs.fr/CAZY/>). The two genes, designated *RGXT1* (At4g01770) and *RGXT2* (At4g01750), were selected for the functional characterization presented here. *RGXT1* and *RGXT2* encode polypeptides of 361 and 367 amino acids, respectively, and are 90% identical at the amino acid level (Figure 1). The two genes are located closely together on chromosome 4, separated by only 6.2 kb. In the *Arabidopsis* genome, many homologous genes are situated in clusters created by recent, local duplications (Coutinho et al., 2003b); thus, it is likely that the two genes are paralogs.

The deduced amino acid sequences of *RGXT1* and *RGXT2* contain a single TMD in the N terminus (36 to 55 in *RGXT1* and 30 to 52 in *RGXT2*; Figure 1) and adopt a type II membrane protein structure typical of Golgi-located GTs (reviewed in Breton et al., 2001). Both proteins contain a DxD motif flanked by hydrophobic residues situated approximately in the middle of the deduced amino acid sequences (190 to 193 in *RGXT1* and 196 to 198 in *RGXT2*; Figure 1), which in several crystal structures has been shown to be the site of interaction with the uridine diphosphate of the donor substrate via a metal cation (Busch et al., 1998; Breton et al., 2001).

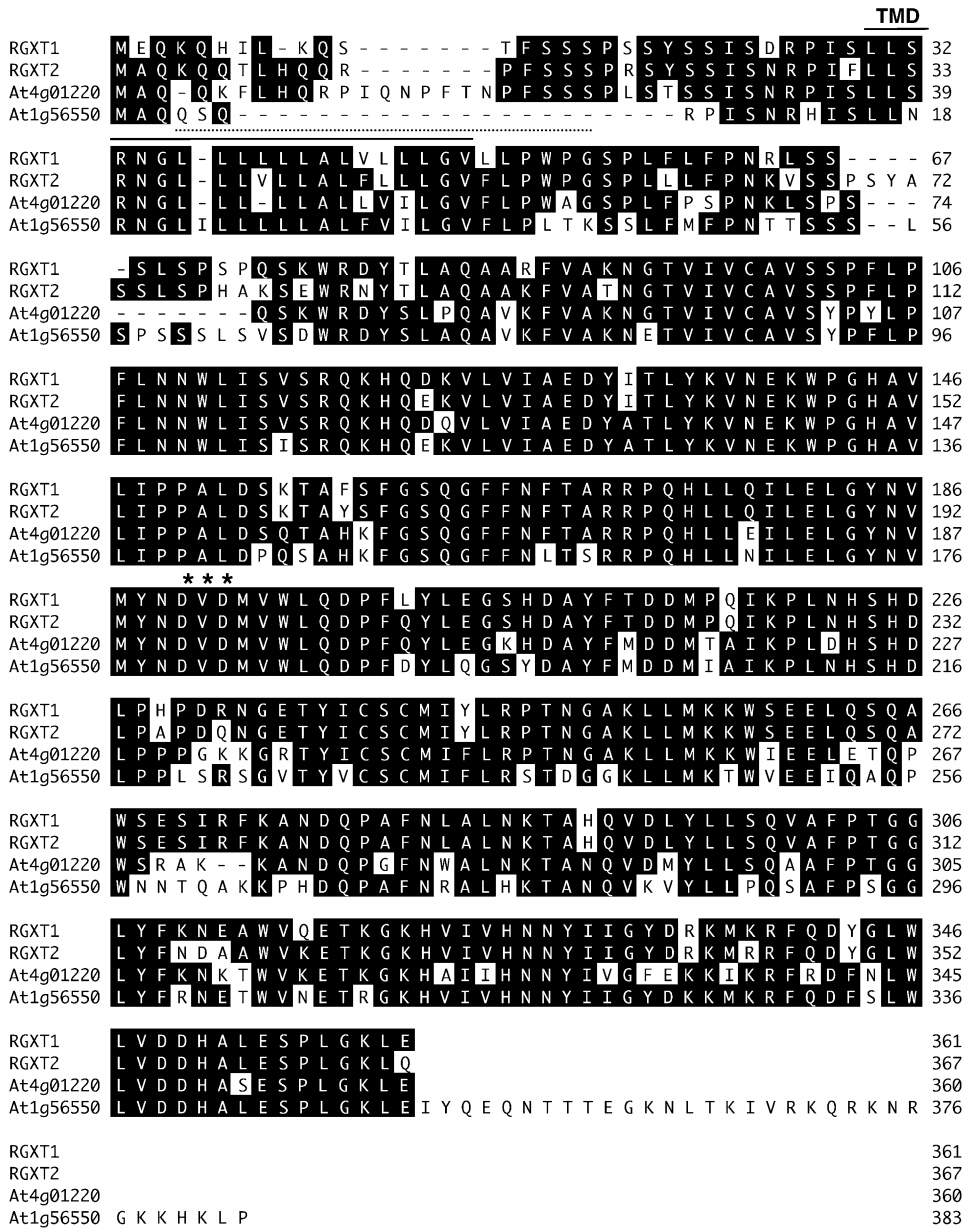


Figure 1. Alignment of the Deduced Amino Acid Sequences of RGXT1 (At4g01770), RGXT2 (At4g01750), and Two Homologous *Arabidopsis* Sequences (At4g01220 and At1g56550).

Position of the predicted TMD is indicated by the line (dotted line for RGXT1 and solid line for RGXT2; Egelund et al., 2004), and the DxD motif involved in the binding of UDP-sugar is indicated with asterisks above the sequence alignment.

Two similar sequences in *Arabidopsis*, At4g01220 and At1g56550, are 68 to 75% identical with RGXT1 and RGXT2 (Figure 1). EST sequences with pronounced similarity to this small gene family have been detected in various plants, for example, *Oryza sativa* (CA763987), *Gossypium arboreum* (BE055585 and BE055834), *Lycopersicon esculentum* (BG124533), *Brassica napus* (BN40062E13), *Beta vulgaris* (BQ487865), *Prunus persica* (BU048490), *Allium cepa* (CF438943), *Citrus sinensis* (CF832864), *Glycine max* (BI969475), *Medicago truncatula* (BI266542), *Populus alba* × *Populus tremula* (CF229735), *Saccharum officinarum*

(CA141232), *Ipomoea nil* (BJ575216), and *Mesembryanthemum crystallinum* (BE034382). Homologous sequences from organisms outside the plant kingdom have not been found.

RGXT1 and RGXT2 Expressed in Baculovirus-Transfected Insect Cells Possess Xylosyltransferase Activity with Fucose as Acceptor

Soluble secreted forms of RGXT1 and RGXT2 were expressed in baculovirus-transfected insect cells (see Supplemental Figure

1 online). One of the main experimental difficulties in determining the catalytic function of GTs relates to the limited availability of relevant candidate oligosaccharide acceptors. However, the range of possible acceptor structures can be narrowed down by exploiting the observation that monosaccharides can serve as acceptor analogs if provided at high concentrations in the GT assay, also denoted as the free sugar assay (Brückner et al., 2000; Wandall et al., 2003). By combining available donor nucleoside diphosphate- ^{14}C -sugars (NDP- ^{14}C -sugars) and monosaccharide acceptors in the free sugar assay, heterologously expressed RGXT1 and RGXT2 protein were shown to catalyze the transfer of D- ^{14}C -xylose (D- ^{14}C -Xyl) from UDP- α -D- ^{14}C -Xyl onto L-fucose (L-Fuc) and with lower efficiency, D- ^{14}C -Xyl onto L-arabinose (L-Ara) (Figure 2A). All other combinations with the donor NDP- ^{14}C -sugars (UDP- α -D- ^{14}C -glucose, UDP- α -D- ^{14}C -galactose, UDP- α -D- ^{14}C -N-acetyl-glucosamine, UDP- α -D- ^{14}C -glucuronic acid, GDP- β -L- ^{14}C -fucose, and GDP- α -D- ^{14}C -mannose) and monosaccharide acceptors (D-glucose [D-Glc], D-galactose [D-Gal], L-rhamnose [L-Rha], D-xylose [D-Xyl], D-mannose, L-Fuc, and N-acetyl-D-glucosamine [D-GlcNAc]) did not result in the formation of radioactive products (data not shown). Thus, both RGXT1 and RGXT2 encode xylosyltransferases using UDP- α -D-Xyl specifically as donor substrate, transferring D-Xyl onto L-Fuc, and less efficiently onto L-Ara. D- ^{14}C -Xyl was only incorporated at high L-Ara concentrations, whereas no transfer occurred at low concentrations (1 to 10 mM) compared with when L-Fuc was used as acceptor (data not shown). Xylose linked to arabinose is a rare epitope in the plant CW and has so far only been found in arabinoxylan of *Cinnamomum zeylanium* (Gowda and Sarathy, 1987). The arabinose residue is in the furanose form (L-Araf) in this case, and L-Araf is generally much more abundant in the CW than arabinose in pyranose form (L-Arap). The equilibrium between L-Araf and L-Arap in the free sugar assay is driven toward L-Arap. To test if L-Araf would work as an efficient acceptor substrate, we chose (1,5)- α -L-arabinobiose as a substrate featuring an L-Araf at the nonreducing end. No incorporation of ^{14}C -xylose was observed (Figure 2A), and we therefore decided to focus on L-Fuc as the acceptor.

Determination of the Disaccharide Linkage

The stereochemistry of the glycosidic linkage of the product obtained after incubation of RGXT2 with UDP- α -D- ^{14}C -Xyl and L-Fuc was determined by treating the product with either α - or β -xylosidase and analyzing the reaction mixture by size exclusion chromatography (SEC; Figure 2B). Only α -xylosidase released D- ^{14}C -Xyl from the product (Figure 2B), showing that RGXT2 is a retaining GT (α -xylosyltransferase). The chemical structure of the product formed in the free sugar assay using methyl α -L-fucoside as acceptor was resolved by nuclear magnetic resonance (NMR). The disaccharide product was purified by mass spectrometry (MS)-guided fractionation using HPLC (see Supplemental Figure 2 online). The peak displaying the expected molecular mass of the sodium adduct ($[\text{M}+\text{Na}]^+$) at a mass-to-charge ratio of 333 was collected and used in the NMR experiments presented in Supplemental Figure 3 online. Both one- (1D) and two-dimensional (2D) spectra were recorded: 1D, ^1H double quantum-filtered correlated spectroscopy ($dq\text{COSY}$);

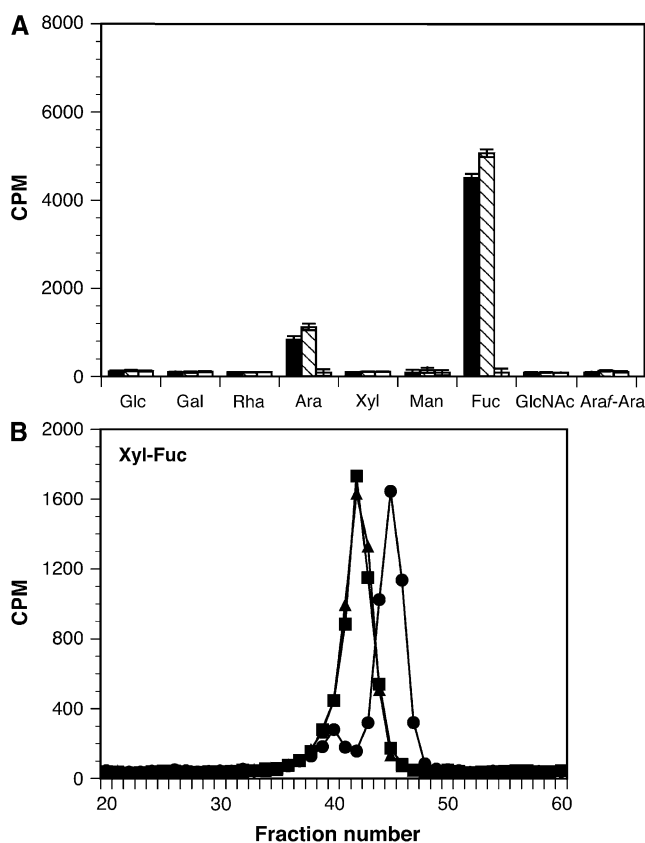


Figure 2. Free Sugar Assay Using UDP- α -D- ^{14}C -Xyl as Donor and 0.5 M Monosaccharide or Disaccharide Acceptors.

(A) Free sugar assay using 100 μM UDP- α -D-Xyl (containing 0.5 μM UDP- α -D- ^{14}C -Xyl $\sim 11,000$ cpm) as donor and 0.5 M monosaccharide or disaccharide acceptors. Supernatant of the baculovirus-transfected High Five cells expressing soluble forms of RGXT1 (closed bars), RGXT2 (hatched bars), and a control construct (open bars) were used in the assays. Averages from three independent experiments are shown \pm SE. Combination of other NDP- ^{14}C -sugars and monosaccharides did not result in any radioactive product. Araf-Ara, 1,5- α -L-arabinobiose.

(B) Product analysis using xylosidases that specifically cleave α - or β -linked D-Xyl. Product produced by combination of UDP- α -D- ^{14}C -Xyl and L-Fuc (Xyl-Fuc) was treated with buffer (squares), *Sulfolobus solfataricus* α -xylosidase (circles), or *Escherichia coli* β -xylosidase (triangles) and analyzed by SEC.

2D, ^1H - ^1H chemical shift correlation, J-resolved spectroscopy (JRES) (2D spectrum with ^1H chemical shift versus coupling constants), heteronuclear single quantum coherence (HSQC; one bond 2D ^{13}C - ^1H chemical shift correlation), and heteronuclear multiple bond correlation (HMBC; multiple bond 2D ^{13}C - ^1H chemical shift correlation). The chemical shifts and coupling constants are given in Table 1. The point of xylose attachment to the fucose moiety was evident from two HMBC cross-peaks, xylose(H1)-fucose(C3) and fucose(H3)-xylose(C1) (see Supplemental Figure 3E online). In addition, there was an 8-ppm downfield shift of C3 in the fucose moiety relative to C3 in unsubstituted methyl α -L-fucoside. The small coupling constant

Table 1. NMR Spectral Data of Methyl α -D-Xylopyranosyl-(1,3)- α -L-Fucopyranoside in D₂O

Position	δ C (ppm)	δ H (ppm)	$^3J_{H,H}$ (Hz)
Fucose moiety			
MeO	56.9	3.34	
1	101.1	4.73	ND ^a
2	68.8	3.92	4.0; 10.4
3	79.9	3.80	3.2; 10.4
4	73.4	3.88	3.2; 1.9
5	68.2	3.99	ND
6	16.7	1.15	6.6
Xylose moiety			
1	102.6	5.09	3.8
2	73.6	3.47	3.8; 9.7
3	74.6	3.66	8.6; 9.7
4	71.1	3.55	ND
5	63.4	3.63 ^b	ND

All data were extracted from ¹H and the 2D NMR spectra.

^a ND, not determined.

^b Same chemical shift for H-5 axial and H-5 equatorial.

of 3.8 Hz of the anomeric xylose proton is diagnostic of the α -linkage. The anomeric proton of the fucose was hidden by the HOD peak, but its coupling constant could be derived at 4.0 Hz from the coupling constants of H2, confirming an untouched α -configuration of the methyl α -L-fucoside. All ¹³C chemical shifts were in acceptable accordance with the monomeric reference compounds methyl α -D-xyloside and methyl α -L-fucoside (Agrawal et al., 1985). The cross-peak at 5.09/63.4 in the HMBC spectrum corresponds to xylose(H1)-xylose(C5), proving that the xylose is in pyranose form, which also can be seen from the ¹³C data, where the shifts are below 80 ppm (xylose in furanose form will have shifts above 80 ppm).

Taken together, the NMR data revealed the regio- and stereochemistry of the methyl xylosyl-fucoside to be an α -(1,3) linkage. The only known plant oligo- or polysaccharide featuring an (1,3)- α -D-linked Xyl-L-Fuc structure is in the A-chain of pectic RG-II (Figure 3B).

Xylosyltransferase Activity on Various Acceptors Containing α -L-Fucose

The α -(1,4) linkage between L-Fuc and L-Rha in the RG-II A-chain prompted us to examine various acceptors containing α -linked L-Fuc (Figure 3A). The smallest possible increment in acceptor size is the methyl fucoside, which comprises a glycosidic bond and at the same time fixes the anomeric configuration. Therefore, methyl α - and β -L-Fuc were chemically synthesized. Methyl α -L-Fuc was found to be an \sim 5 times more efficient acceptor than free L-Fuc, whereas methyl β -L-Fuc did not lead to any D-[¹⁴C]-Xyl incorporation (Figure 3A). Thus, the preference for an α -glycosidic bond of L-Fuc appeared to be absolute as acceptor for both RGXT1 and RGXT2. The next obvious acceptor increment, the α -L-Fuc-(1,4)-L-Rha disaccharide, was prepared by chemical synthesis, and this acceptor was found to be a slightly better acceptor than free L-Fuc. To investigate the possible

influence of the anomeric configuration of the L-Rha moiety, the methyl glycosides of the disaccharide, methyl α -L-fucosyl-(1,4)- α -L-rhamnoside [methyl α -L-Fuc-(1,4)- α -L-Rha], and methyl α -L-fucosyl-(1,4)- β -L-rhamnoside [methyl α -L-Fuc-(1,4)- β -L-Rha] were synthesized and tested as acceptors. Both worked 1 to

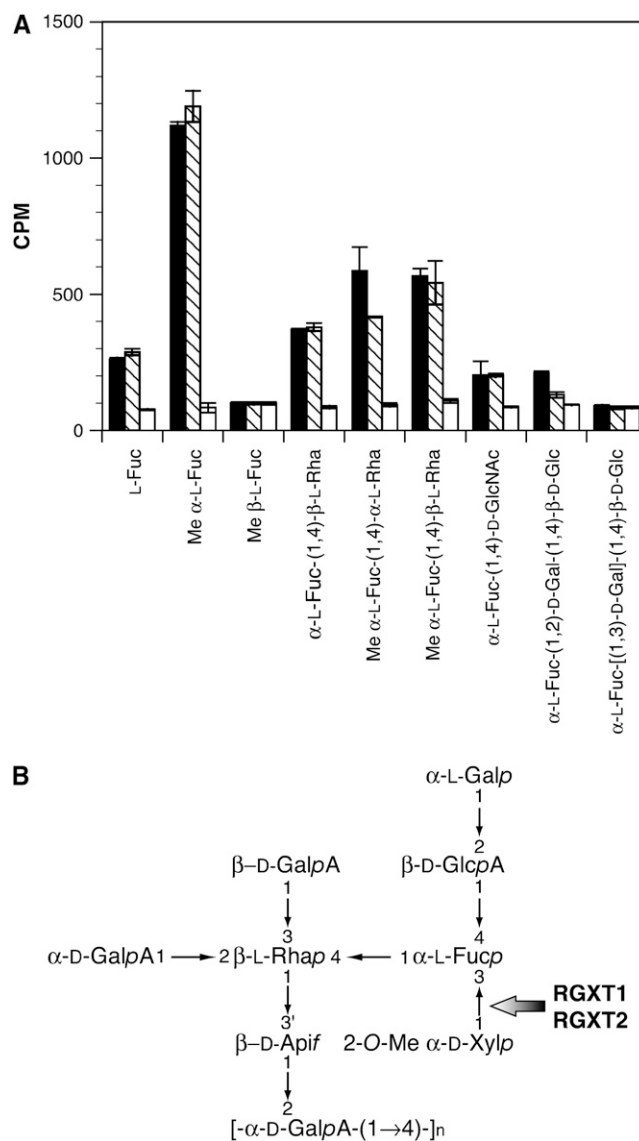


Figure 3. Xylosyltransferase Activity of RGXT1 and RGXT2 Using Different Acceptors.

(A) Supernatants of the baculovirus-transfected High Five cells expressing soluble forms of RGXT1 (closed bars), RGXT2 (hatched bars), and a control construct (open bars) were incubated with 100 μ M UDP- α -D-Xyl (containing 0.5 μ M UDP- α -D-[¹⁴C]-Xyl \sim 11,000 cpm) and 1 mM of each acceptor: L-Fuc, methyl α -L-Fuc; methyl β -L-Fuc, α -L-Fuc-(1,4)-L-Rha, methyl α -L-Fuc-(1,4)- α -L-Rha, methyl α -L-Fuc-(1,4)- β -L-Rha, α -L-Fuc-(1,4)-D-GlcNAC, α -L-Fuc-(1,2)-D-Gal-(1,4)- β -D-Glc, and α -L-Fuc-[(1,3)-D-Gal]-(1,4)- β -D-Glc. Averages from three independent experiments are shown \pm SE.

(B) Model of the structure for pectin RG-II A-chain. Predicted site of action of RGXT1 and RGXT2 is indicated by an arrow.

1.5 times better than α -L-Fuc-(1,4)-L-Rha, but no significant differences were found between the α - and β -forms of the methyl glycosides (Figure 3A). α -L-Fuc-(1,4)-D-GlcNAc, which features the same linkage as α -L-Fuc-(1,4)-L-Rha, was approximately half as efficient as α -L-Fuc-(1,4)-L-Rha (Figure 3A). The two fucosyl-D-lactose trisaccharides, in which α -L-Fuc is conjugated to either the D-Gal or D-Glc residue at the O-2' or O-3 position, respectively, were found to be less efficient acceptors than α -L-Fuc-(1,4)-D-GlcNAc (Figure 3A). In conclusion, RGXT1 and RGXT2 prefer L-Fuc being α -linked to the O-4 position of the adjacent sugar over linkages to the O-2 and O-3 positions. The level of incorporation of D-[14 C]-Xyl onto α -L-Fuc-(1,4)-L-Rha was one-third of the incorporation obtained with methyl α -L-Fuc (Figure 3A), which is somewhat unexpected, given the predicted involvement of RGXT1 and RGXT2 in the synthesis of the α -D-Xyl-(1,3)- α -L-Fuc-(1,4)-L-Rha structure in RG-II. Possible explanations for this apparent discrepancy are presented in the Discussion.

Monosaccharide Composition of CWs from T-DNA Insertional Mutants of *RGXT1* and *RGXT2*

If both RGXT1 and RGXT2 are involved in the synthesis of the RG-II A-chain and the two genes do not fully complement one another, mutants harboring T-DNA insertion in either *RGXT1* or *RGXT2* might feature a RG-II population in which the methylated

D-Xyl residue (2-O-methyl D-Xyl) is reduced or missing. T-DNA insertional mutants for *RGXT1* (Salk_073748) and *RGXT2* (Salk_023883) with insertions in the last exon and in the first intron of the two genes, respectively (Figure 4A), as determined by sequencing from the T-DNA left border (Alonso et al., 2003) were selected for this investigation. Three (*rgxt1-5*, *rgxt1-8*, and *rgxt1-10*) and two (*rgxt2-4* and *rgxt2-6*) homozygous plants for mutation of *RGXT1* and *RGXT2*, respectively, were identified by PCR (Figure 4B), the phenotype scored, and the sugar composition of the CW fractions determined. No obvious morphological differences between the wild type and mutants were observed. The 2-O-methyl D-Xyl residue is diagnostic of RG-II and could be detected in alcohol-insoluble residues (AIRs) from rosette leaves by gas chromatography electro-ionization (GC/EI)-MS, but the concentration was too low to permit precise quantification. RG-II-enriched preparations were therefore made from the wild type and mutants and analyzed. The sugar composition from the isolated RG-II revealed that no statistically significant changes were caused by the T-DNA insertion in either *RGXT1* or *RGXT2* (Table 2). Apparently, the mutation in either gene did not eliminate the 2-O-methyl D-Xyl residue, probably because the other gene product compensated for the dysfunction of the mutated xylosyltransferase gene. A similar case has been observed for T-DNA insertional mutants of UDP- α -D-Api/UDP- α -D-xylose synthase (*AXS1*), of which *Arabidopsis* contains at least two homologous genes (Ahn et al., 2006).

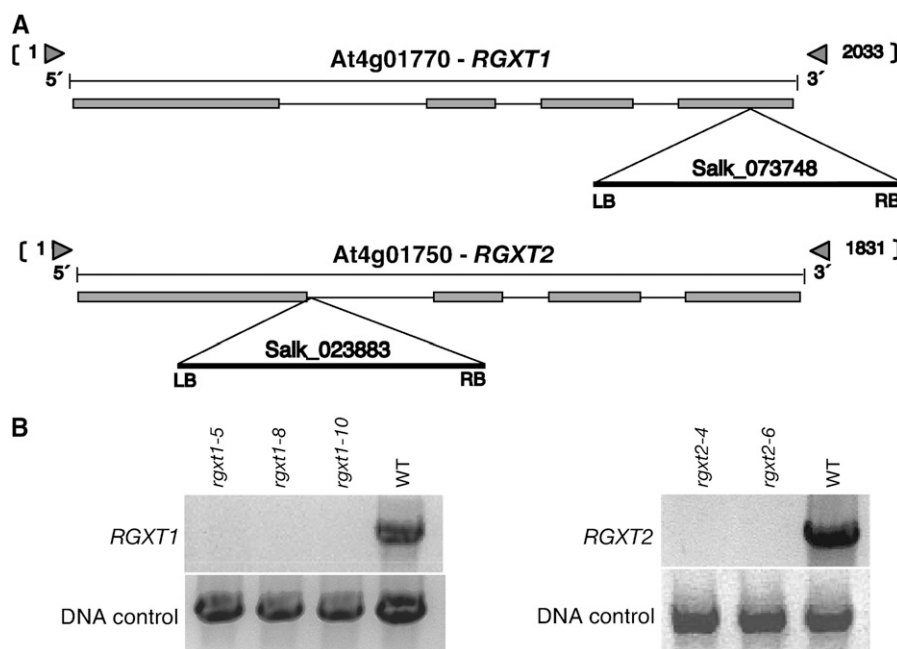


Figure 4. T-DNA Insertional Mutants in *RGXT1* and *RGXT2*.

(A) Positions of the T-DNA insertions in the *RGXT1* and *RGXT2* genes. Boxes indicate exons, and lines indicate introns. The T-DNA is inserted in the last exon in *RGXT1* (Salk_073748) and in the first intron in *RGXT2* (Salk_023883).

(B) Three (*rgxt1-5*, *rgxt1-8*, and *rgxt1-10*) and two (*rgxt2-4* and *rgxt2-6*) homozygous plants were identified for *RGXT1* and *RGXT2*, respectively, using PCR with genomic DNA as the template and a set of gene-specific primers outside the T-DNA insertions. "DNA control" refers to the amplification of At1g75120. Similar results were obtained in the next generation (data not shown).

Table 2. Sugar Composition of RG-II Isolated from Wild-Type and T-DNA Insertional Mutants of *RGXT1* and *RGXT2*

Genotype	Wild Type	<i>rgxt1</i>	<i>rgxt2</i>
MeFuc	3.4 ± 0.4	3.1 ± 0.4	2.7 ± 0.8
Rha	13.2 ± 0.5	14.0 ± 1.7	11.2 ± 2.6
Fuc	3.0 ± 0.7	3.7 ± 0.5	3.5 ± 0.3
MeXyl	4.9 ± 0.3	4.7 ± 0.3	4.0 ± 1.0
Ara	14.3 ± 1.8	16.2 ± 1.6	14.1 ± 1.2
Ace	2.7 ± 0.2	1.9 ± 0.1	2.9 ± 0.8
Api	8.5 ± 3.7	4.8 ± 0.6	3.5 ± 1.1
Gal	10.2 ± 1.5	15.6 ± 3.7	12.9 ± 2.3
GlcA	6.3 ± 0.1	2.5 ± 0.6	3.0 ± 0.3
GalA	30.4 ± 1.7	31.6 ± 3.1	39.4 ± 3.8
Dha	3.3 ± 2.2	2.0 ± 0.3	3.0 ± 0.9
Kdo ^a	ND ^b	ND	ND

Molar percentages of each sugar residue analyzed by GC and GC/EL-MS. The values are shown as the average of three independent experiments ± SE.

^a Kdo, detected but not quantified due to background interference.

^b ND, not determined.

Xylosyltransferase Activity with the Mutant RG-II as Acceptor Substrate

Radiochemical transferase assays are more sensitive than chemical analysis of monosaccharide profiles, and it was therefore decided to characterize the mutant RG-IIs for their ability to serve as acceptor substrates. The preparations of RG-II from the wild type, *rgxt1*, and *rgxt2* listed in Table 2 were used for acceptor substrate studies. Both *RGXT1* and *RGXT2* catalyzed transfer of D-[¹⁴C]-Xyl to the RG-II preparation from the *rgxt1* T-DNA insertional mutant plants (~1000 cpm above incorporation into wild-type RG-II; Figure 5A) and at a higher level to RG-II from the *rgxt2* T-DNA insertional mutant plants (~3000 cpm above incorporation into wild-type RG-II; Figure 5B). α -Xylosidase very efficiently removed *RGXT2*-incorporated D-[¹⁴C]-Xyl from the RG-II of both T-DNA insertional mutants (Figures 5A and 5B). Wild-type RG-II did not work as an acceptor (Figures 5A and 5B), and a control insect supernatant containing the soluble secreted form of CAZy GT-family-77 At1g75110 did not transfer D-[¹⁴C]-Xyl to the mutant RG-IIs (Figures 5A and 5B).

In conclusion, the mutant RG-IIs were not identical to the wild-type counterpart, although the differences were below the detection limits of our chemical analysis, and both *RGXT1* and *RGXT2* catalyzed the transfer of D-[¹⁴C]-Xyl to RG-II isolated from both T-DNA insertional mutants, which suggests that *RGXT1* and *RGXT2* are xylosyltransferases involved in the synthesis of the α -D-Xyl-(1,3)- α -L-Fuc-(1,4)-L-Rha structure in pectic RG-II.

Expression Profile of *RGXT1* and *RGXT2*

The levels of *RGXT1* and *RGXT2* transcripts in various tissues were investigated using RT-PCR. Whereas a strong 18S rRNA derived band was obtained (18S in Figure 6), neither *RGXT1*- nor *RGXT2*-derived transcripts were detectable after 25 cycles of PCR (data not shown). After 45 cycles of PCR amplification, both *RGXT1* and *RGXT2* mRNAs were detected (Figure 6). *RGXT1*

mRNA was found in root and rosette leaves, and *RGXT2* was detected in root, rosette leaves, stem, and flower (Figure 6) and generally appeared to be expressed at a higher level.

RNA gel blot analysis was not sensitive enough to detect the transcripts in any of the selected tissues (data not shown). BLAST searches with the *RGXT1* and *RGXT2* cDNA sequences at the National Center for Biotechnology Information (NCBI;

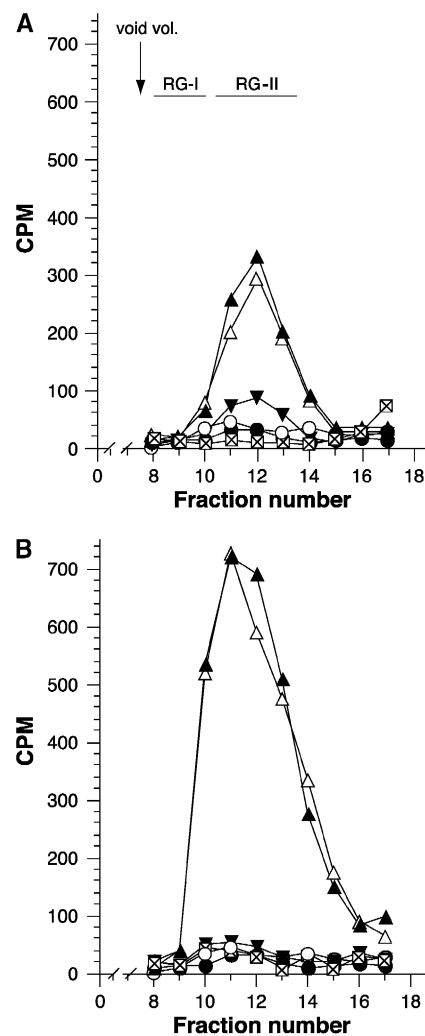


Figure 5. Xylosyltransferase Activity of Heterologously Expressed *RGXT1* and *RGXT2* Using RG-II Acceptor Substrates Prepared from *rgxt1*, *rgxt2*, and the Wild Type.

Supernatant of the baculovirus-transfected High Five cells expressing soluble forms of *RGXT1* (open symbols), *RGXT2* (closed symbols), and the control construct (boxed X symbols) were incubated with 100 μ M UDP- α -D-Xyl (containing 2.0 μ M UDP- α -D-[¹⁴C]-Xyl ~44,000 cpm) and RG-II (100 μ g) isolated from either the wild type (circles), mutants (triangles), or mutants post-treated with α -xylosidase (inverted triangles) and separated by SEC.

(A) RG-II isolated from *rgxt1* and the wild type.

(B) RG-II isolated from *rgxt2* and the wild type. A total of ~1000 cpm (2.3%) and ~3000 CPM (6.8%) of the radiolabeled donor were incorporated into RG-II from *rgxt1* and -2, respectively.

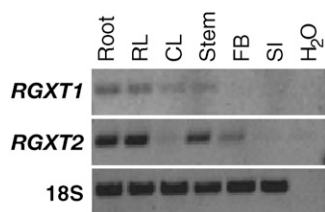


Figure 6. Expression Analysis of *RGXT1* and *RGXT2* by RT-PCR.

RT-PCR was performed with specific primer sets for *RGXT1* (45 PCR cycles), *RGXT2* (45 PCR cycles), or for ribosomal 18S as control (25 PCR cycles) on root, rosette leaves (RL), cauline leaves (CL), stem, flower buds (FB), and siliques (SI) from 4-week-old wild-type plants. Water was included as a control. Each RT-PCR reaction was performed twice to ensure reproducibility.

<http://www.ncbi.nlm.nih.gov>) revealed the existence of a limited number of ESTs derived from root, leaf, flower, seedlings, and mixed tissues of various developmental stages (data not shown). The ESTs could rarely be assigned with certainty to *RGXT1* or *RGXT2* because of the high similarity of the two genes.

Subcellular Location of *RGXT1* and *RGXT2*

The subcellular location of *RGXT1* and *RGXT2* was investigated by C-terminal fusions of the full-length coding regions to the enhanced green fluorescent protein (EGFP) and EGFP alone as a control (Figure 7A). After biolistic particle bombardments of wild-type *Arabidopsis* rosette leaves, cells expressing the *RGXT1*-EGFP protein (Figures 7B and 7D) displayed GFP fluorescence in small vesicles similar to those of other Golgi-localized enzymes (Staelin and Driouich, 1997). The same pattern was observed for the *RGXT2*-EGFP fusion protein (data not shown). Expression of EGFP alone showed diffused fluorescence in the cytosol and in particular in the cytoplasm surrounding the nucleus (data not shown), a clearly distinct pattern from that of *RGXT1*-EGFP protein.

The fluorescent structures were investigated further by treatment with Brefeldin A (BFA). BFA is a lipophilic fungal toxin known to block vesicular transport in the secretory pathway between the endoplasmic reticulum and the Golgi and between Golgi and the trans-Golgi network. In some cases, BFA also induces vesiculation and disassembly of the Golgi apparatus (Staelin and Driouich, 1997; Ritzenthaler et al., 2002). When cells were treated with BFA, the labeling pattern in the *RGXT1*-EGFP bombarded cells changed from a clear pattern of well-defined bodies in the untreated control (Figures 7B and 7D) to a pattern of diffuse and disassembled vesicles (Figures 7C and 7E) as would be expected for Golgi-localized proteins. A similar difference between treated and untreated cells was observed for *RGXT2*-EGFP (data not shown). Golgi location was further corroborated using a ceramide stain recommended for labeling the Golgi apparatus in plants (Ruzin, 1999). BODIPY TR ceramide produces selective staining of the Golgi complex and can easily be observed by confocal laser scanning microscopy (CLSM) (Nadia et al., 2002). BODIPY TR staining of transgenic *Arabidopsis* cells expressing the *RGXT1*-EGFP fusion protein (Figures 7F

and 7G) matched perfectly when the two images were merged (Figure 7H), showing that the fusion protein colocalized with the BODIPY TR dye. Again, similar results were obtained with *RGXT2*-EGFP (data not shown). In conclusion, both the BFA and the BODIPY TR results are consistent with targeting to the Golgi apparatus.

DISCUSSION

The pectic matrix is coextensive with the cellulose-hemicellulose network and can transmit stresses in the wall (McCann and Roberts, 1994) but has generally not been considered to be a major load-bearing structure. However, the recent finding by Zykwinska et al. (2005) that both galactan and to a lesser extent arabinan side chains of RG-I bind specifically to cellulose lead the authors to propose a CW model in which the cellulose microfibrils are tethered by parallel networks of hemicellulose and pectin. The significance of RG-I side chains to physical wall properties have been shown by Jones et al. (2003) and Ulvskov et al. (2005). The structural significance of RG-II to CW integrity and cell-cell adhesion is well established, and the measurements of tensile strength of wild-type and mutant CWs by Ryden et al. (2003) showed that both xyloglucan cross-linking and RG-II borate complex formation are essential for wall strength. The interest of the scientific community in unraveling the biosynthesis and assembly of the pectic matrix is therefore intense, and recent, successful gene discovery efforts have led to the identifications of the first GTs with roles in pectin biosynthesis. Our identification of *RGXT1* and *RGXT2* is an important step toward unraveling the synthesis of RG-II, which, with its unique glycosidic linkages and rare monosaccharides, remains a major challenge.

Sequence Analysis

The results presented in this article show that both *RGXT1* and *RGXT2* encode (1,3)- α -D-xylosyltransferases. *RGXT1* and *RGXT2* are novel and do not appear to be related to other known (1,3)- α -GTs, such as the human blood group A (1,3)- α -N-acetylgalactosaminyltransferase, assigned to CAZy GT-family-6, or the α -(1,6)- or the (1,2)- β -D-xylosyltransferases involved in the xyloglucan and N-glycan biosynthesis and assigned to CAZy GT-family-34 and -61, respectively. *RGXT1* and *RGXT2* were thus used to seed CAZy GT-family-77, which presently comprises 34 accessions: 18 from *Arabidopsis*, 15 from *O. sativa*, and a single *Dictyostelium discoideum* (1,3)- α -D-galactosyltransferase (Ketcham et al., 2004), which also catalyzes the formation of an α -(1,3)-linkage to fucose. Classification of a GT to a particular CAZy family is very strong evidence for catalytic mechanism, retaining or inverting, and the type of linkage formed generally also correlates well with family membership. Classification to a family usually does not allow predictions about acceptor substrate, and we will not make inferences from the fact that all three known activities transfer to a fucosyl residue. However, it is likely that the formation of (1,3)-linkages is typical of the GT-family-77 enzymes.

Gene families involved in CW polysaccharide modification and disassembly are often quite large, while most GTs appear to

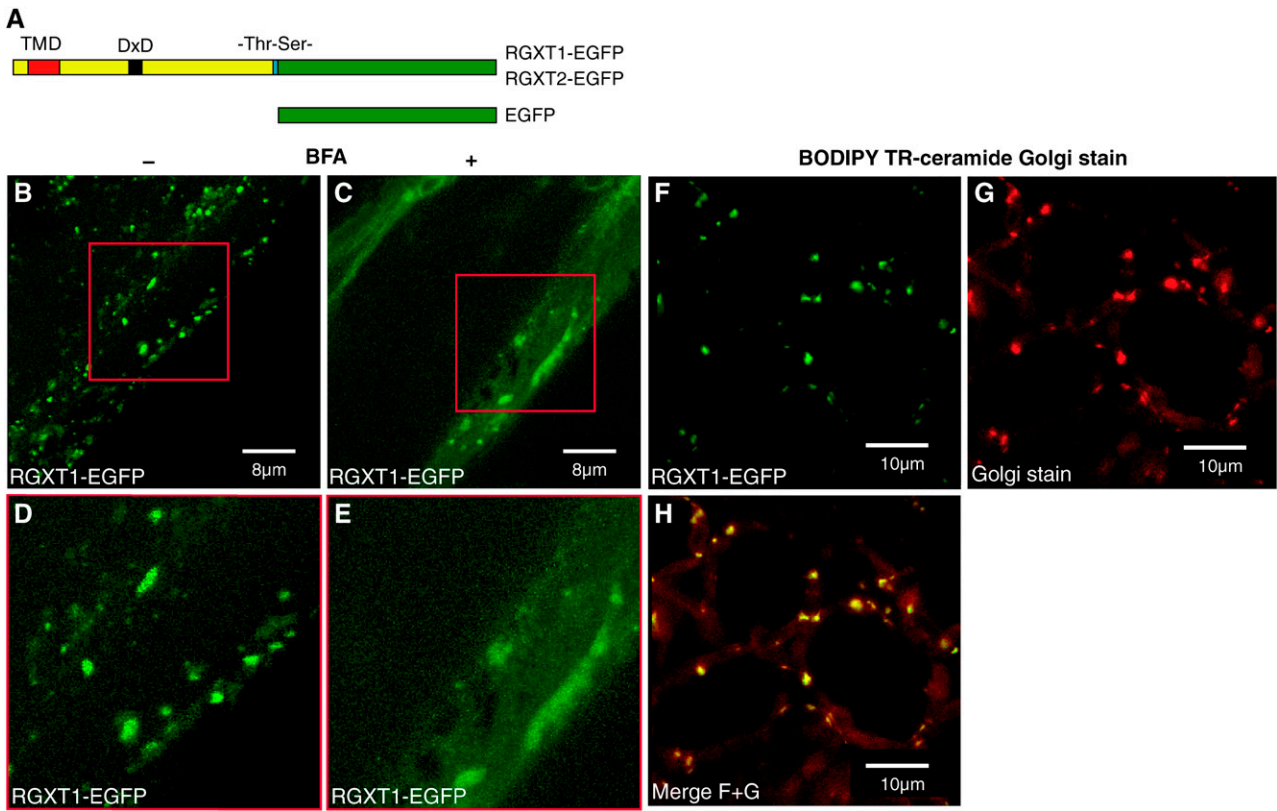


Figure 7. Subcellular Location of RGXT1-EGFP Fusion Protein in *Arabidopsis* Epidermal Cells after Biolistic Particle Delivery Analyzed by CLSM.

- (A) Structures of native EGFP and fusion proteins of RGXT1-EGFP and RGXT2-EGFP.
 (B) to (H) CLSM-derived images.
 (C) and (E) Effect of BFA treatment on RGXT1-EGFP location.
 (B) Fluorescence from RGXT1-EGFP is associated with multiple vesicles.
 (C) Fluorescence obtained after BFA treatment.
 (D) Close-up of the region indicated in (B).
 (E) Close-up of the region indicated in (C). BFA treatment changed the pattern of EGFP fluorescence in the defined vesicles [(B) and (D)] to diffuse and possibly partly disassembled vesicles [(C) and (E)].
 (F) to (H) Cells expressing RGXT1-EGFP stained with BODIPY TR ceramide.
 (F) Fluorescence from the RGXT1-EGFP fusion protein.
 (G) Fluorescence from the BODIPY TR ceramide.
 (H) Merged images of (F) and (G) showing that the RGXT1-EGFP fusion protein colocalizes with the BODIPY TR ceramide. RGXT2-EGFP protein showed a similar fluorescence pattern (data not shown).

occur as single genes or in very small gene families. *RGXT1* and *RGXT2* are quite similar members of CAZy GT-family-77, but their gene family may have additional members. The *Arabidopsis* sequences At4g01220 and At1g56550 are 68 to 75% identical to *RGXT1* and *RGXT2* and share the same overall protein structure, containing a TMD region close to the N terminus and a DxD motif with hydrophobic surroundings (Figure 1). They form a separate phylogenetic cluster with the two xylosyltransferases (data not shown) but have not yet been proven to be fucose-specific xylosyltransferases. The 16 remaining *Arabidopsis* accessions in GT-family-77 display low sequence identities with *RGXT1* and *RGXT2* (19% or lower), and we consider these to be too distantly related to allow inferences about their catalytic function. It will be interesting to see if the xylosyltransferases constitute a gene

family with four members. It may, in this case, require an RNA interference strategy that affects all family members to effectively interfere with the biosynthesis of the RG-II polysaccharide.

Protein Structure and Subcellular Localization

Both proteins encoded by *RGXT1* and *RGXT2* are predicted to adopt the topology of typical type II membrane proteins. It has been known for a long time that noncellulosic polysaccharides are synthesized in the Golgi apparatus (Ray et al., 1969), and enzymes involved in the synthesis of the backbone of noncellulosic β -linked CW polysaccharides (e.g., the mannan synthases) have been shown to be Golgi localized, multimembrane-spanning enzymes (Dhugga et al., 2004; Liepman et al., 2005).

Evidence pointing toward pectin also being synthesized in the Golgi has been reviewed by Staehelin and Moore (1995), and it has since then been substantiated by biochemical evidence that three enzymes involved in pectin biosynthesis are bound to the Golgi membrane with the active site facing the lumen (Goubet and Mohnen, 1999; Sterling et al., 2001; Geshi et al., 2004). It is therefore very likely that RG-II is also assembled in the Golgi vesicles, which is supported by the accumulation of RGXT1-EGFP and RGXT2-EGFP fusion proteins in an intracellular compartment that disintegrates upon treatment with BFA. The results are comparable to those obtained by Burget et al. (2003), who used BFA treatment to determine the Golgi location of the MUR4-GFP fusion protein in *Arabidopsis* cells.

Enzymatic Activity and Expression

Characterization and assignment of function to GTs is often impeded by technical difficulties related to design of suitable biochemical assays. The free sugar assay employed in this study allowed a first insight into the nature of the catalytic activity. Soluble versions of both RGXT1 and RGXT2 expressed in insect cells transferred D-Xyl from UDP- α -D-Xyl to methyl α -L-Fuc. The mass and structure of the resulting disaccharide was determined using liquid chromatography (LC)/MS and the NMR data unequivocally demonstrate the formation of an α -(1,3) linkage to the methyl xylosyl fucoside. The activity, transferring D-Xyl from UDP- α -D-Xyl onto L-Fuc, is unique, since L-Fuc is normally a terminal sugar. In plants, L-Fuc is present as terminal sugar [α -L-Fuc-(1,2)- β -D-Gal-(1 \rightarrow)] in both RG-II, RG-I (Ridley et al., 2001), and xyloglucan (Perrin et al., 2003), as [L-Fuc-(1,3)- β -D-GlcNAc-(1 \rightarrow)] in N-glycans (Lerouge et al., 1998), and as [α -L-Fuc-(1,2)- α -L-Ara-(1 \rightarrow)] in some arabinogalactan proteins (van Hengel and Roberts, 2002). The only known internal fucose is located in the A-chain of RG-II [α -L-Fuc-(1,4)- β -L-Rha-(1 \rightarrow)], the proposed target of the Np *GUT1* gene product (Iwai et al., 2002) and the *RGXT1* and *RGXT2* gene products. Given the complexity of plant CW polysaccharides, it cannot be ruled out that other polysaccharide structures containing an internal fucose are yet to be discovered.

Xylosyltransferases that take part in RG-II A-chain biosynthesis transfer very little carbon into the CW, and a very low level of expression is to be expected, perhaps even lower than the fucosyltransferase involved in xyloglucan biosynthesis (Sarria et al., 2001). Unfortunately, a high-resolution RT-PCR expression profile of *RGXT1* and *RGXT2* cannot be determined when 45 cycles are required, but the expression profiles are in reasonable agreement with the EST sequences reported so far.

Insertional Mutants, Phenotype, and Source of Acceptor Substrate

The complete RG-II molecule from T-DNA insertional mutants was isolated with the dual purpose of determining the mutant wall phenotype and recovering a RG-II acceptor substrate lacking the D-Xyl residue. The glycosyl residue composition of RG-II isolated from both *rgxt1* and *rgxt2* did not differ significantly from wild-type RG-II (Table 2). This is attributed to complementation because both *RGXT1* and *RGXT2* are expressed in all

major tissues. The data presented in Table 2 may, however, suggest a subtle effect of the mutations on the RG-II structure, with possible differences in D-GlcA content, which may be relevant given that the only RG-II D-GlcA is linked to the A-chain fucosyl residue. It should be noted, however, that the mutant level of D-GlcA is in accordance with the generally accepted RG-II model, while the wild-type D-GlcA level is slightly higher than expected, though well within range of the D-GlcA level found in wild-type *Arabidopsis* by Reuhs et al. (2004). The overall differences between wild-type and mutant RG-IIs are too small to be assessed precisely. However, heterologously expressed *RGXT1* and *RGXT2* were able to discriminate between wild-type and mutant RG-II where chemical analysis could not and specifically catalyzed transfer of xylose only to the mutant RG-II. These results suggest that RG-II occurs as a mixture of wild-type and mutant RG-II in both mutants. The *RGXT2* insertional mutant yielded a more effective acceptor substrate than the *RGXT1* mutant, suggesting that the more strongly expressed *RGXT2* better complements the weakly expressed *RGXT1* than vice versa.

The chemically synthesized methyl α -L-Fuc with a fixed anomeric center was found to be a better acceptor than L-Fuc, whereas the synthesized methyl β -L-Fuc did not act as acceptor. These findings are in full agreement with the predicted structure

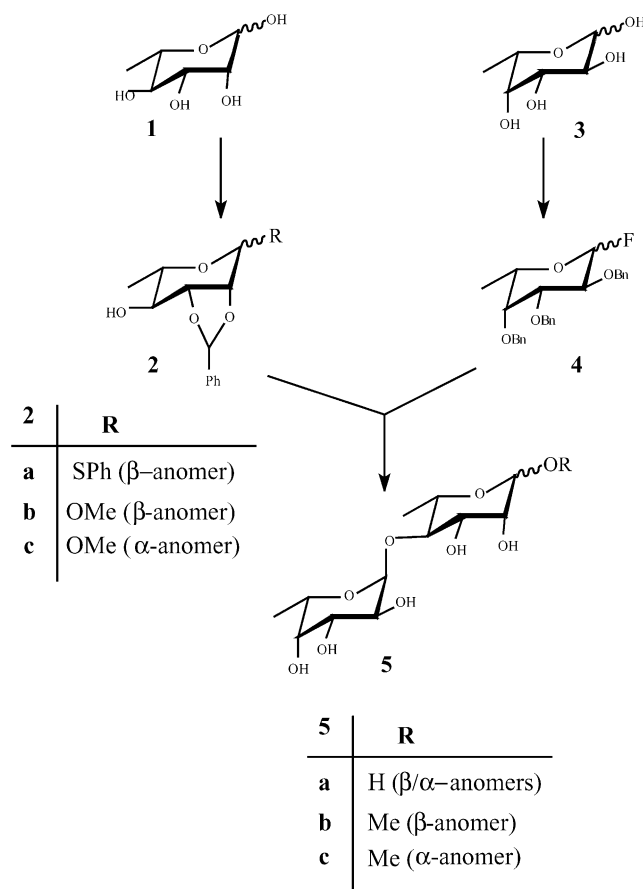


Figure 8. Pathway for Chemical Synthesis of α -L-Fucopyranosyl-(1,4)- α/β -L-Rhamnopyranose and Its Methyl Glycosides.

of the A-chain in RG-II being the site of action for RGXT1 and RGXT2. The α -L-Fuc-(1,4)-L-Rha disaccharide and its methyl glycosides were synthesized to obtain acceptors that represent a bigger part of the A-chain than the monosaccharides, L-Fuc and methyl α -L-Fuc. The three disaccharides were all better acceptors than L-Fuc, but surprisingly none of them were better than methyl α -L-Fuc. One interpretation would be that the acceptor substrate is indeed incorrectly assigned. This would entail that the RG-II preparations should contain small amounts of an impurity that represent an unknown polysaccharide featuring an internal α -L-Fuc in the wild-type case. We consider this unlikely, and a comparison of our monosaccharide profiles in Table 2 with a state-of-the-art characterization of *Arabidopsis* RG-II (Reuhs et al., 2004) clearly shows that authentic RG-II was used in the acceptor assays. Other explanations should therefore be considered.

The biosynthetic steps forming the A-chain are not known, but the process must necessarily be tightly regulated, since the A-chain is conserved in all examined vascular plants. The three adjacent sugar residues to L-Fuc in the A-chain are L-Rha, 2-O-Me-D-Xyl, and D-GlcA. L-Fuc is believed to be attached to L-Rha first due to the direction of synthesis of the chain growing from the nonreducing end. Then, with our results in mind, one could speculate that D-GlcA may have to be added to α -L-Fuc-(1,4)- β -L-Rha before 2-O-Me-D-Xyl. However, the study of the glucuronosyltransferase (Np *GUT1*) by Iwai et al. (2002) argues against this explanation, since their mutant lacks D-GlcA (and the L-galactose attached to the D-GlcA), while 2-O-Me-D-Xyl is present. Another possible explanation regards the conformation of the growing A-chain, which may be fixed during synthesis in another conformation than the preferred conformation of the free disaccharide, which would thus encounter steric hindrance in the active site that methyl α -L-Fuc would not experience. Ketcham et al. (2004) made analogous observations with the CAZy GT-family-77 *D. discoideum* galactosyltransferase, where a trisaccharide substrate analog was inferior as acceptor compared with the corresponding disaccharide and the α -L-Fuc methyl glycoside acceptor. The authors propose that the fucosyl residue folds back in the trisaccharide but is prevented from doing so in the native glycoprotein acceptor, hence rendering the trisaccharide a poorer than expected acceptor analog. We hypothesize that similar conformational issues apply to the RG-II A-chain. More insight to this hypothesis could be obtained by use of larger acceptors, but such are not readily available today.

The precise monosaccharide sequences of the RG-II side chains may be faithfully conserved by targeting the participating enzymes to early or later compartments in the Golgi as well as by the formation of complexes within the particular compartment. Several members of the GAUT family are predicted to be targeted to the Golgi but are lacking membrane anchors (Sterling et al., 2006). The Np *GUT1* gene product is similarly predicted to have an incomplete membrane anchor, and its targeting to the site of RG-II synthesis in the Golgi may thus rely on protein-protein interactions and the formation of a complex that synthesizes the RG-II A-chain. With the identification of *RGXT*, two different members of the hypothetical complex are known and can be used to address important questions about the assembly of a very complex, yet fully conserved CW building block.

METHODS

Growth Conditions of *Arabidopsis thaliana* Plants

Arabidopsis thaliana ecotype Columbia (Col-0; wild type) and T-DNA insertional mutant plants were grown in soil in a controlled-environment growth chamber (Percival AR-60 I) at a photosynthetic flux of 100 to 120 $\mu\text{mol photons m}^{-2} \text{s}^{-1}$ at an 8-h-light/16-h-dark cycle, 20°C, and 70% relative humidity. Glass house-grown plants were used for large-scale RG-II preparation.

Enzymes, Chemicals, and Reagents

α -Xylosidase was a kind gift from Marco Moracci (Institute of Protein Biochemistry and Enzymology, Consiglio Nazionale delle Ricerche, Naples, Italy). *Escherichia coli* β -xylosidase was from Sigma-Aldrich. UDP- α -D-[^{14}C]-Glc, UDP- α -D-[^{14}C]-Gal, UDP- α -D-[^{14}C]-GlcNAc, GDP- β -L-[^{14}C]-Fuc, and GDP- α -D-[^{14}C]-Man were from Amersham Biosciences (GE-Healthcare). UDP- α -D-[^{14}C]-GlcA and UDP- α -D-[^{14}C]-Xyl were from NEN. UDP- α -D-Xyl was from CarboSource (Complex Carbohydrate Resource Center), and other non-isotope-labeled nucleoside diphosphate sugars were from Calbiochem-Novabiochem. The disaccharide (1,5)- α -L-arabinobiose was from Megazyme International. Other chemicals and reagents were from Sigma-Aldrich.

Chemical Synthesis of Methyl α -L-Fucoside, Methyl β -L-Fucoside, α -L-Fuc-(1,4)-L-Rha, and Its Methyl Glycosides

Methyl α -L-fucopyranoside and methyl β -L-fucopyranoside were prepared using a modification of the Fischer method (Deriaz et al., 1949) in which L-Fuc was heated with 1.25 M methanolic hydrogen chloride at 80°C and the reaction followed by thin layer chromatography until the starting material had disappeared. Subsequently, the reaction product was acetylated using acetic anhydride-sodium acetate to enhance chromatographic separation of the formed anomeric mixture (chromatographic separation was performed on silica gel column using the eluent system of 10% acetone in *n*-pentane). The obtained methyl 2,3,4-tri-O-acetyl- α -L-fucopyranoside was deacetylated using sodium methoxide in methanol to provide the desired methyl α -L-fucopyranoside.

The strategy for synthesis of α -L-fucopyranosyl-(1,4)-L-rhamnopyranose (5a) and its methyl glycosides (5b and 5c) is outlined in Figure 8, which involves the conversion of L-Rha (1) into the suitable glycosyl acceptors (2a to 2c) and the conversion of L-Fuc (3) into a suitable glycosyl donor (4). Recently, we reported a short and practical methodology for conversion of unprotected sugars into the corresponding phenyl 4,6-O-benzylidene-per-O-acetylated-1,2-*trans*-thioglycosides (Larsen et al., 2003). This protocol was successfully applied to convert L-Rha (1) into the glycosyl acceptors 2,3-O-benzylidene- β -L-rhamnopyranoside derivatives (2a to 2c). Based on the same approach, L-Fuc was modified and converted in five steps into the glycosyl donor 2,3,4-tri-O-benzyl- α - β -L-fucopyranosyl fluoride (4). The glycosidation reaction between (2a to 2c) and (4) was achieved using the activator silver perchlorate-tin dichloride system (Mukaiyama et al., 1981), and subsequent deprotection led to the desired products (5a to 5c).

All intermediates were purified to homogeneity and their structures ascertained by ^1H and ^{13}C NMR spectroscopy. Experimental details and proof of the identity of the synthesized products will be published elsewhere.

Cloning of *RGXT1* and *RGXT2* cDNAs

RGXT1 (At4g01770) was cloned by RT-PCR from total RNA isolated from roots of 4-week-old bolting *Arabidopsis* plants using the following primer set: forward primer (5'-ATGGAGCAGAAACAACATATTC-3') and reverse

primer (5'-TTACTCTAATTTCCCTAATGGAG-3'). Total RNA was extracted using TRIzol reagent (Invitrogen) according to the manufacturer's instructions. RT-PCR was performed according to Mikkelsen et al. (2003), with the exception of the cycle parameters in the PCR, which were as follows: 3 min at 94°C, 45 cycles of 94°C for 30 s, 50°C for 30 s, and 68°C for 30 s, followed by 12 min at 72°C. *RGXT2* (At4g01750) was cloned by PCR from a λ YES cDNA library (Elledge et al., 1991) using the following primer set: forward primer (5'-ATACGGATCCGAACAAGTCTCTCTCCTT-3') and reverse primer (5'-ATGAGCGGCCGCTTACTGCAATTTCCCTAATGGA-3'). The amplified full-length cDNA coding sequences were cloned into the pUC18 vector using the *Sma*I site.

Heterologous Expression in Insect Cells

Fragments corresponding to the soluble forms of the proteins (i.e., amino acid residues 56 to 361 of *RGXT1* and 53 to 367 of *RGXT2*) were PCR amplified using the forward primers 5'-CATACACGTGGATCCTTCTCCTTATTCTGTTTCCA-3' for *RGXT1* and 5'-CATAGGATCCTTGGCCCGGATCTCCTTTGTT-3' for *RGXT2*, the reverse primers 5'-ATGACCGCGGGCGGCCGCTTACTCTAATTTCCCTAATGG-3' for *RGXT1* and 5'-TGATGACCGCGGGCGGCCGCTTACTGCAATTTCCCTAATGGA-3' for *RGXT2* (restriction sites *Bam*HI, *Sac*II, and *Not*I are underlined), and the full-length cDNAs as a template. The PCR products were cloned into the pBKS-HISTAG II vector (a kind gift from Eric Paul Bennett, University of Copenhagen) in frame with an N-terminal hexa-histidine tag, thrombin cleavage site, and T7 affinity tag using the restriction sites *Bam*HI (5'-end) and *Sac*II (3'-end). The pBKS-HISTAG II vector is a modified pBluescript SK +/- vector carrying the following extra sequences in between *Eco*RI-*Bam*HI sites: 5'-GAAATTCGCGGCCGAGCAGCCATCATCATCATCACAGCAGCGGCTGGTGGCGCGGCCGAGCCATATGGCTAGCATGACTGGTGGACAGCAAATGGATCC-3' (underlined italics indicate *Eco*RI and *Bam*HI sites, and the rest of the underlined nucleotides (5' to 3' direction) encode six histidines, a thrombin cleavage site [LVPRGS], and the T7 affinity tags [MASMTGGQMD]). Finally, the tag-gene fusions were isolated using a *Not*I site and cloned into the pAcGP67A vector (BD Biosciences Pharmingen) in frame with the leader peptide. All constructs were fully sequenced.

pAcGP67A containing soluble, tagged forms of *RGXT1* and *RGXT2* was cotransfected with Baculo-Gold DNA (BD Biosciences Pharmingen) and virus amplified as described by Bennett et al. (1996). Enzyme assay was performed with supernatant containing the secreted enzymes of transfected Sf9 and High Five cells. Insect supernatant containing the soluble secreted form of the At1g75110 gene product was used as control.

Immunoblot Analysis

Samples containing 30 μ g of protein were boiled for 10 min and then separated on a 10% SDS polyacrylamide gel. Proteins were then transferred to a nitrocellulose membrane as recommended by the manufacturer (Sigma-Aldrich) and probed with a peroxidase-conjugated antibody against the his-tag (A7058 from Sigma-Aldrich). The signal was detected using chemiluminescence. An identical gel was stained with Comassie Brilliant Blue R 250 to ensure equal loading.

Enzyme Assay

The free sugar assay was performed according to Brückner et al. (2000) with the following modifications. Standard assays were performed in 50 μ L of reaction mixture containing 25 mM ammonium formate, pH 7.5, 10 mM MnCl₂, 100 μ M NDP-sugar, including \sim 0.5 μ M NDP-[¹⁴C]-sugar (200 to 300 mCi/mmol, \sim 10 nCi/ μ L, 9.8 GBq/mmol, 1 nCi = 2.2×10^3 cpm, yielding a total of \sim 11,000 cpm in the assay), 0.5 M monosaccharide, and 2 μ L of supernatant of High Five cells after transfection of the *RGXT1*- or *RGXT2*-containing construct. For acceptor studies using

L-Fuc and L-Fuc derivatives, 1 mM of each acceptor and 10 μ L of High Five supernatant was used. After incubation for 1 h at 30°C, unincorporated NDP-[¹⁴C]-sugar was removed by passing the reaction mixture through a Dowex-1 anion exchanger (1X8, 200 to 400 mesh Cl; Sigma-Aldrich), and the radioactivity in the flow through was determined by scintillation counting.

Xylosyltransferase assay using isolated RG-II as acceptor was performed in 50 μ L of reaction mixture containing 100 mM ammonium formate, pH 7.5, 10 mM MnCl₂, 100 μ M unlabeled UDP- α -D-Xyl, including \sim 2.0 μ M radiolabeled UDP- α -D-[¹⁴C]-Xyl (200 to 300 mCi/mmol, \sim 10 nCi/ μ L, 9.8 GBq/mmol, 1 nCi = 2.2×10^3 cpm, yielding a total of \sim 44,000 cpm in the assay), \sim 100 μ g RG-II, and 10 μ L High Five supernatant, which was incubated for 4 h at 30°C with shaking. Incorporated α -D-[¹⁴C]-Xyl from RG-II was released with α -xylosidase as described below. The products were separated using a Superdex Peptide column (30-cm long, 1-cm i.d.; Pharmacia GE-Healthcare) eluted with 50 mM ammonium formate, pH 5.0, at a flow rate of 24 mL/h. Fractions were collected in 2-min intervals (0.8 mL), and the radioactivity was determined by scintillation counting.

Product Analysis by α - and β -Xylosidase Treatment

RGXT2 in the High Five supernatant was incubated with a combination of UDP- α -D-[¹⁴C]-Xyl and L-Fuc by scaling up the standard free sugar assay 10-fold. After incubation, unincorporated NDP-[¹⁴C]-sugar and enzyme was removed by anion exchange chromatography as described above. The products were dried, dissolved in 50 mM sodium acetate, pH 5.0, and divided into three aliquots. Each aliquot was incubated with 2 milliunits α -xylosidase (Moracci et al., 2000) or β -xylosidase (X1378; Sigma-Aldrich). Incubation was performed at the optimal temperature for each enzyme (70°C for 5 h for α -xylosidase and control, and 37°C for 5 h for β -xylosidase). The enzyme digests and an undigested control were separated on the Superdex Peptide column eluted with 50 mM ammonium formate, pH 5.0, at a flow rate of 24 mL/h. Fractions were collected in 1-min intervals (0.4 mL) and the radioactivity was determined by scintillation counting.

Structural Characterization of the Methyl Xyl-Fuc Disaccharide

For preparative purposes (NMR), an upscaled and unlabeled version of the free sugar assay was used, containing 1 mM UDP- α -D-Xyl and 1 mM methyl α -L-Fuc in 5 mL. The incubation was extended to 96 h, and *RGXT2* was added in aliquots at 0, 24, 48, and 72 h to ensure a high yield. After incubation, unincorporated UDP- α -D-Xyl and enzyme were removed by anion exchange chromatography as described above. The flow-through was concentrated and dissolved in water, and the reaction mixture was further purified using an HR16/60 column packed with Sephadex G10 (Pharmacia GE-Healthcare) and eluted with water at a rate of 40 mL/h. The relevant fractions, previously determined using radioactively labeled product, were combined, lyophilized, and applied to MS-guided HPLC. LC-MS was performed on an Agilent 1100 Series LC (Agilent Technologies) coupled to a Bruker Esquire 3000+ ion trap mass spectrometer (Bruker Daltonics). For preparative isolation of the disaccharide, an amino column (Macherey-Nagel CC 123/3 Nucleosil 100-3 NH₂, 125 \times 3 mm, 3 μ m) was used at a flow rate of 0.5 mL \cdot min⁻¹. The mobile phases were as follows: A, 5 μ M NaCl, 0.1% formic acid; B, 100% acetonitrile. An unknown precipitate following the addition of acetonitrile was removed by centrifugation before applying the sample to the HPLC column. The preparative chromatography was performed isocratically at 95% solvent B and 5% solvent A. The fraction centered at 9.0 min displaying a strong [M+Na]⁺ at a mass-to-charge ratio of 333 was collected. After evaporation, the sample was dissolved in D₂O and analyzed by NMR on a Bruker Avance 400 instrument using an inverse probe (BBI). The ¹H frequency was at 400.1 and ¹³C at 100.6 MHz. ¹H and ¹³C chemical shifts were

based on dioxane as internal reference [$\delta_H(\text{dioxane}) = 3.75$; $\delta_C(\text{dioxane}) = 67.4$]. The available amount of material was too low to allow recording of 1D ^{13}C or distortionless enhancement by polarization transfer spectra; therefore, all chemical shifts were extracted from the 2D spectra (*dq*COSY, JRES, HSQC, and HMBC). To achieve an appropriate HMBC spectrum, 1120 transients in each of the 128 spectra in the F1 dimension were recorded over 90 h. Although the isolated sample contained ~20% of an unknown impurity, unambiguous identification could be done.

Analysis of CWs from T-DNA Insertional Mutants in *RGXT1* and *RGXT2*

T-DNA insertional mutants in *RGXT1* (Salk_073748) and *RGXT2* (Salk_023883) were obtained from the Nottingham Arabidopsis Stock Centre (Alonso et al., 2003). Homozygous plants were identified by two PCRs. In the first PCR, a pair of gene-specific primers designed to anneal outside of the T-DNA insertion were used, which in case of homozygosity does not produce a band of the predicted size (negative selection): forward primer 5'-ATGGAGCAGAAACAACATATTC-3' for *RGXT1* and 5'-ATGGCGCAGAAACAACAG-3' for *RGXT2* and reverse primer 5'-TTACTCTAATTTCCCTAATGGAG-3' for *RGXT1* and 5'-TTACTGCAATTTCCCTAATG-3' for *RGXT2*. As a positive control of the negative selection, a set of At1g75120-specific primers (5'-ATGGCGGTTTCGTAAGAG-3' forward and 5'-CTATGAACCATCACGGAAC-3') unrelated to *RGXT1* and *RGXT2* were used to amplify a fragment of the expected size. Genomic DNA was isolated using the Nucleon PhytoPure kit (Amersham Biosciences). In the subsequent PCR, the T-DNA left border-specific primer (5'-AGCGTGGACCGCTTGCTGCAACT-3') in combination with one of the gene-specific primers (positive selection) was used.

RG-II was isolated from AIR prepared from rosette leaves of 4-week-old wild-type and mutant plants according to the method described by Ishii et al. (2001). For 100 mg of AIR, 20 units of EPG (Megazyme International) were used. EPG digests were separated on a 25 mm \times 30 cm Superdex 75 column at a flow rate of 6 mL/min. RG-II containing fractions were treated with 0.5 μL of Novozymes *Aspergillus niger* pectinase (Sigma P2736, no activity declared) for 3 h at room temperature, freeze dried, and purified on the Superdex Peptide column as described for the xylosyltransferase assay above. RG-II-containing fractions to be used in acceptor assays were combined and dialyzed before concentration by freeze-drying. For the purpose of determinations of monosaccharide, profile dialysis was omitted and the lyophilizate was redissolved in water and freeze-dried three times to remove ammonium formate. The monosaccharide composition was determined by GC and GC-MS analysis of the alditol acetate derivatives for neutral sugar composition analysis and methanolysis and trimethylsilylation derivatives for neutral and acidic sugar composition analysis (York et al., 1985).

Transcript Detection by RT-PCR

RNA was extracted from root, rosette leaves, cauline leaves, stem, siliques, and flower from 4-week-old bolting *Arabidopsis* plants grown as described above. RT-PCR was performed according to Mikkelsen et al. (2003). The following primer sets were used to amplify each transcript specifically: *RGXT1* forward, 5'-TTATCGGTTACGACAGGAAA-3'; *RGXT1* reverse, 5'-TTCTACTAAACATTACAAC-3'; *RGXT2* forward, 5'-TATCGGTTACGATAGGAAA-3'; *RGXT2* reverse, 5'-TGTTTCTACTAAACATTACAA-3'; 18S forward, 5'-TAAGGATTGACAGACTGAGA-GCT-3'; and 18S reverse, 5'-AATACATCAGTGTAGCGCGCT-3'.

Localization of *RGXT1*- and *RGXT2*-EGFP Fusion Proteins

C-Terminal fusions of the coding regions of *RGXT1* and *RGXT2* to EGFP under control of the 35S promoter were obtained using the pCambia 1301 vector (CAMBIA). The *gusA* gene in pCambia 1301 was cut out with *NcoI*

and *BstEII* and replaced with EGFP amplified by PCR using the forward primer 5'-ATATCCATGGCACTAGTATGGTGGAGCAAGGGCGAGGAGC-3', reverse primer 5'-ATATGGTCACCTTACGTTTCTCGTTCAGC-3', and the pPZP111-EGFP (EGFP from pEGFP; Clontech) vector as template. Subsequently, the entire coding region of *RGXT1* or *RGXT2* was PCR amplified using the forward primer 5'-ATATGGATCCCCATGGAGCA-GAAACAACATAT-3' for *RGXT1*, 5'-ATATGGATCCCCATGGCGCAGAAACAACAGA-3' for *RGXT2* and reverse primer 5'-ATATACTAGTCTC-TAATTTCCCTAATGGAG-3' for *RGXT1* and 5'-ATATACTAGTCTGCAA-TTCCCTAATGGAG-3' for *RGXT2* and inserted in frame with the 5'-end of the EGFP sequence by cloning into the *NcoI* and *SpeI* sites, introducing two extra amino acids (Thr and Ser, indicated in Figure 7A) in the junction between the coding regions of *RGXT1*, *RGXT2*, and *EGFP*. The constructs were introduced into rosette leaves of *Arabidopsis* using biolistic particle bombardment (Helios Gene Gun; Bio-Rad) according to Helenius et al. (2000). Twenty-four hours after delivery, fluorescent epidermal cells were identified using CLSM (Leica DMREX; Leica Microsystems) with argon/krypton laser excitation. EGFP-derived fluorescence was detected using an excitation wavelength of 488 nm with the emission wavelength at 505 to 520 nm. For subcellular location studies, the bombarded rosette leaves were treated for 2 h with 100 $\mu\text{g mL}^{-1}$ BFA (Sigma-Aldrich) or water as control. To confirm reproducibility of the observations, multiple cells from independent experiments were examined. BODIPY TR ceramide (Molecular Probes) stainings were performed following the manufacturer's protocols. For colocalization of EGFP and BODIPY TR, a 488-nm argon/krypton laser and a 633-nm helium/neon laser were used simultaneously, as described by Nadia et al. (2002).

Accession Numbers

Sequence data from this article can be found in the NCBI data library under the following accession numbers: *RGXT1*, BK005829 (locus At4g01770); and *RGXT2*, BK005830 (locus At4g01750).

Supplemental Data

The following materials are available in the online version of this article.

Supplemental Figure 1. Immunoblot Analysis of Histidine-Tagged *RGXT1* and *RGXT2* Protein Expressed in High Five Cells.

Supplemental Figure 2. MS-Guided HPLC Purification of the Product Obtained after Incubation of UDP- α -D-Xyl and Methyl α -L-Fucopyranoside with *RGXT2*.

Supplemental Figure 3. NMR Spectra of Methyl α -D-Xylopyranosyl-(1,3)- α -L-Fucopyranoside in D_2O (Sample from Supplemental Figure 2).

ACKNOWLEDGMENTS

We thank Marco Moracci (Consiglio Nazionale delle Ricerche, Naples, Italy), Ronald W. Davis (Stanford University School of Medicine, Stanford, CA), and Barbara A. Halkier (Royal Veterinary and Agricultural University) for providing the α -xylosidase, λYES library, and pPZP111-EGFP vector, respectively. We also thank Eric Paul Bennett (University of Copenhagen), Kirsten Nielsen (Royal Veterinary and Agricultural University), and Michael Hansen (Royal Veterinary and Agricultural University) for help with insect cell expression and CLSM. Kenneth Keegstra (Michigan State University) is acknowledged for his collaborative initiatives early in this project, and William G.T. Willats (University of Copenhagen) is thanked for helpful suggestions. We thank Vibeke Strange Petersen, Dorthe Christiansen, and Winnie Dam for their skillful technical assistance. This work was supported by the Danish National Research Foundation (B.L.P., M.S.M., C.E.O., P.U., and N.G.), the

Ministry of Science, Technology, and Innovation (I.D.), PROBRAIN (T.I.), and the Danish Medical Research Council (H.C.).

Received July 29, 2005; revised August 23, 2006; accepted September 18, 2006; published October 20, 2006.

REFERENCES

- Agrawal, P.K., Jain, D.C., Gupta, R.K., and Thakur, R.S. (1985). Carbon-13 NMR spectroscopy of steroidal saponinins and steroidal saponins. *Phytochemistry* **24**, 2479–2496.
- Ahn, J.-W., Verma, R., Kim, M., Lee, J.-Y., Kim, Y.-K., Bang, J.-W., Reiter, W.-D., and Pai, H.-S. (2006). Depletion of UDP-D-apiose/UDP-D-xylose synthases results in rhamnogalacturonan-II deficiency, cell wall thickening, and cell death in higher plants. *J. Biol. Chem.* **281**, 13708–13716.
- Alonso, J.M., et al. (2003). Genome-wide insertional mutagenesis of *Arabidopsis thaliana*. *Science* **301**, 653–657.
- Bennett, E.P., Hassan, H., and Clausen, H. (1996). cDNA cloning and expression of a novel human UDP-N-acetyl-alpha-D-galactosamine. Polypeptide N-acetylgalactosaminyltransferase, GalNAc-T3. *J. Biol. Chem.* **271**, 17006–17012.
- Bouton, S., Leboeuf, E., Mouille, G., Leydecker, M.T., Talbot, J., Granier, F., Lahaye, M., Hofte, H., and Truong, H.N. (2002). QUA-SIMODO1 encodes a putative membrane-bound glycosyltransferase required for normal pectin synthesis and cell adhesion in *Arabidopsis*. *Plant Cell* **14**, 2577–2590.
- Breton, C., Mucha, J., and Jeanneau, C. (2001). Structural and functional features of glycosyltransferases. *Biochimie* **83**, 713–718.
- Brückner, K., Perez, L., Clausen, H., and Cohen, S. (2000). Glycosyltransferase activity of Fringe modulates Notch-Delta interactions. *Nature* **406**, 411–415.
- Burget, E.G., Verma, R., Mølhøj, M., and Reiter, W.-D. (2003). The biosynthesis of L-arabinose in plants: Molecular cloning and characterization of a Golgi-localized UDP-D-xylose 4-epimerase encoded by the *MUR4* gene of *Arabidopsis*. *Plant Cell* **15**, 523–531.
- Busch, C., Hofmann, F., Selzer, J., Munro, S., Jeckel, D., and Aktories, K. (1998). A common motif of eukaryotic glycosyltransferases is essential for the enzyme activity of large Clostridial cytotoxins. *J. Biol. Chem.* **273**, 19566–19572.
- Coutinho, P.M., Deleury, E., Davies, G.J., and Henrissat, B. (2003a). An evolving hierarchical family classification for glycosyltransferases. *J. Mol. Biol.* **328**, 307–317.
- Coutinho, P.M., Stam, M., Blanc, E., and Henrissat, B. (2003b). Why are there so many carbohydrate-active enzyme-related genes in plants? *Trends Plant Sci.* **8**, 563–565.
- Deriaz, R.E., Overend, W.G., Stacey, M., and Wiggins, L.F. (1949). Deoxysugars. Part VI. The constitution of β -methyl-2-deoxy-L-ribo-pyranoside and α/β -methyl-2-deoxy-L-ribo-pyranoside. *J. Chem. Soc.* 2836–2841.
- Dhugga, K.S., Barreiro, R., Whitten, B., Stecca, K., Hazebroek, J., Randhawa, G.S., Dolan, M., Kinney, A.J., Tomes, D., Nichols, S., and Anderson, P. (2004). Guar seed beta-mannan synthase is a member of the cellulose synthase super gene family. *Science* **303**, 363–366.
- Doong, R.L., Liljebjelke, L., Fralish, G., Kumar, A., and Mohnen, D. (1995). Cell free synthesis of pectin: Identification and partial characterization of polygalacturonate 4- α -galacturonosyltransferase and its products from membrane preparations of tobacco cell suspension cultures. *Plant Physiol.* **109**, 141–152.
- Egelund, J., Skjøt, M., Geshi, N., Ulvskov, P., and Petersen, B.L. (2004). A complementary bioinformatic approach to identify potential plant cell wall glycosyltransferase encoding genes. *Plant Physiol.* **136**, 2609–2620.
- Elledge, S.J., Mulligan, J.T., Ramer, S.W., Spottswood, M., and Davis, R.W. (1991). λ YES: A multifunctional cDNA expression vector for the isolation of genes by complementation of yeast and *Escherichia coli* mutants. *Proc. Natl. Acad. Sci. USA* **88**, 1731–1735.
- Fleischer, A., O'Neill, M.A., and Ehwald, R. (1999). The pore size of non-graminaceous plant cell walls is rapidly decreased by borate ester cross-linking of the pectin polysaccharide rhamnogalacturonan II. *Plant Physiol.* **121**, 829–838.
- Geshi, N., Jørgensen, B., and Ulvskov, P. (2004). Subcellular location and topology of β (1-4)galactosyltransferase that elongates β (1-4)galactan side chains in rhamnogalacturonan I in potato. *Planta* **218**, 862–868.
- Goubet, F., and Mohnen, D. (1999). Subcellular location and topology of homogalacturonan methyltransferase in suspension-cultured *Nicotiana tabacum* cells. *Planta* **209**, 112–117.
- Gowda, D.C., and Sarathy, C. (1987). Structure of an L-arabino-D-xylan from the bark of *Cinnamomum zeylanicum*. *Carbohydr. Res.* **166**, 263–269.
- Harholt, J., Jensen, J.K., Sørensen, S.O., Orfila, C., Pauly, M., and Scheller, H.V. (2006). Arabinan deficient 1 is a putative arabinosyltransferase involved in biosynthesis of pectic arabinan in *Arabidopsis*. *Plant Physiol.* **140**, 49–58.
- Helenius, E., Boije, M., Niklander-Teeri, V., Palva, E.T., and Teeri, T.H. (2000). Gene delivery into intact plants using the Helios™ Gene Gun. *Plant Mol. Biol. Rep.* **18**, 287–288.
- van Hengel, A.J., and Roberts, K. (2002). Fucosylated arabinogalactan-proteins are required for full root cell elongation in *Arabidopsis*. *Plant J.* **32**, 105–113.
- Ishii, T., and Matsunaga, T. (1996). Isolation and characterization of a boron-rhamnogalacturonan II complex from cell walls of sugar beet pulp. *Carbohydr. Res.* **284**, 1–9.
- Ishii, T., Matsunaga, T., and Hayashi, N. (2001). Formation of rhamnogalacturonan II-borate dimer in pectin determines cell wall thickness of pumpkin tissue. *Plant Physiol.* **126**, 1698–1705.
- Ishii, T., Matsunaga, T., Pellerin, P., O'Neill, M.A., Darvill, A.G., and Alberheim, P. (1999). Plant cell wall polysaccharide rhamnogalacturonan II self-assembles into a covalently cross-linked dimer. *J. Biol. Chem.* **274**, 13098–13109.
- Iwai, H., Masaoka, N., Ishii, T., and Satoh, S. (2002). A pectin glucuronosyltransferase gene is essential for intercellular attachment in the plant meristem. *Proc. Natl. Acad. Sci. USA* **99**, 16319–16324.
- Jones, L., Milne, J.L., Ashford, D., and McQueen-Mason, S.J. (2003). Cell wall arabinan is essential for guard cell function. *Proc. Natl. Acad. Sci. USA* **100**, 11783–11788.
- Ketcham, C., Wang, F., Fisher, S.Z., Ercan, A., van der Wel, H., Locke, R.D., Sirajud-Doula, K., Matta, K.L., and West, C.M. (2004). Specificity of a soluble UDP-galactose:fucoside α -1,3-galactosyltransferase that modifies the cytoplasmic glycoprotein Skp1 in *Dictyostelium*. *J. Biol. Chem.* **279**, 29050–29059.
- Kobayashi, M., Matoh, T., and Azuma, J. (1996). Two chains of rhamnogalacturonan II are cross-linked by borate-diol ester bonds in higher plant cell walls. *Plant Physiol.* **110**, 1017–1020.
- Lao, N.T., Long, D., Kiang, S., Coupland, G., Shoue, D.A., Carpita, N.C., and Kavanagh, T.A. (2003). Mutation of a family 8 glycosyltransferase gene alters cell wall carbohydrate composition and causes a humidity-sensitive semi-sterile dwarf phenotype in *Arabidopsis*. *Plant Mol. Biol.* **53**, 687–701.
- Larsen, K., Olsen, C.E., and Motawia, M.S. (2003). A facile protocol for direct conversion of unprotected sugars into phenyl 4,6-O-benzylidene-per-O-acetylated-1,2-trans-thioglycosides. *Carbohydr. Res.* **338**, 199–202.

- Lerouge, P., Cabanes-Macheteau, M., Rayon, C., Fischette-Laine, A.C., Gomord, V., and Faye, L. (1998). N-glycoprotein biosynthesis in plants: Recent developments and future trends. *Plant Mol. Biol.* **38**, 31–48.
- Liepman, A.H., Wilkerson, C.G., and Keegstra, K. (2005). Expression of cellulose synthase-like (*Cs*) genes in insect cells reveals that *Cs*/A family members encode mannan synthases. *Proc. Natl. Acad. Sci. USA* **102**, 2221–2226.
- Matsunaga, T., Ishii, T., Matsumoto, S., Higuchi, M., Darvill, A.G., Albersheim, P., and O'Neill, M.A. (2004). Occurrence of the primary cell wall polysaccharide rhamnogalacturonan II in pteridophytes, lycophytes, and bryophytes. Implications for the evolution of vascular plants. *Plant Physiol.* **134**, 339–351.
- McCann, M.C., and Roberts, K. (1994). Changes in cell wall architecture during cell elongation. *J. Exp. Bot.* **45**, 1683–1691.
- Mikkelsen, M.D., Petersen, B.L., Glawishnig, E., Jensen, A.B., Andersson, E., and Halkier, B.S. (2003). Modulation of CYP79 genes and glucosinolate profiles in *Arabidopsis* by defense signaling pathways. *Plant Physiol.* **131**, 298–308.
- Moracci, M., Cobucci-Ponzano, B., Trincone, A., Fusco, S., De Rosa, M., van Der Oost, J., Sensen, C.W., Charlebois, R.L., and Rossi, M. (2000). Identification and molecular characterization of the first alpha-xylosidase from an *Archaeon*. *J. Biol. Chem.* **275**, 22082–22089.
- Mukaiyama, T., Murai, Y., and Shoda, S. (1981). An efficient method for glycosylation of hydroxyl compounds using glucopyranosyl fluoride. *Chem. Lett.* **3**, 431–432.
- Nadia, V., Rebecca, S.H., and Donald, L.J. (2002). Identification and characterization of a *Drosophila melanogaster* ortholog of human beta 1,4-galactosyltransferase VII. *Glycobiology* **12**, 589–597.
- O'Neill, M.A., Darvill, A.G., and Albersheim, P. (1990). The pectic polysaccharides of primary cell walls. In *Methods in Plant Biochemistry*, 2nd ed, P.M. Dey, ed (London: Academic Press), pp. 415–441.
- O'Neill, M.A., Eberhard, S., Albersheim, P., and Darvill, A.G. (2001). Requirement of borate cross-linking of cell wall rhamnogalacturonan II for *Arabidopsis* growth. *Science* **294**, 846–849.
- O'Neill, M.A., Warrenfeltz, D.W., Katesm, K., Pellerin, P., Doco, T., Darvill, A.G., and Albersheim, P. (1996). Rhamnogalacturonan II, a pectic polysaccharide in the walls of growing plant cell, forms a dimer that is covalently cross-linked by a borate ester. *J. Biol. Chem.* **271**, 22923–22930.
- O'Neill, M.A., and York, W.S. (2003). The composition and structure of plant primary cell walls. In *Annual Plant Reviews*, J.K.C. Rose, ed (Oxford, UK: CRC Press), pp. 1–54.
- Orfila, C., Sørensen, S.O., Harholt, J., Geshi, N., Crombie, H., Truong, H.-N., Reid, J.S.G., Knox, J.P., and Scheller, H.V. (2005). Quasimodo1 is expressed in vascular tissue of *Arabidopsis thaliana* inflorescence stems, and affects homogalacturonan and xylan biosynthesis. *Planta* **222**, 613–622.
- Perrin, R.M., Jia, Z., Wagner, T.A., O'Neill, M.A., Sarria, R., York, W.S., Raikhel, N.V., and Keegstra, K. (2003). Analysis of xyloglucan fucosylation in *Arabidopsis*. *Plant Physiol.* **132**, 768–778.
- Popper, Z.A., and Fry, S.C. (2003). Primary cell wall composition of bryophytes and charophytes. *Ann. Bot. (Lond.)* **91**, 1–12.
- Ray, P.M., Shiniger, T.L., and Ray, M.M. (1969). Isolation of beta-glucan synthetase particles from plant cells and identification with Golgi membranes. *Proc. Natl. Acad. Sci. USA* **64**, 605–612.
- Reuhs, B.L., Glenn, J., Stephens, S.B., Kim, J.S., Christie, D.B., Glushka, J.G., Zablackis, E., Albersheim, P., Darvill, A.G., and Neill, M.A. (2004). L-Galactose replaces L-fucose in the pectic polysaccharide rhamnogalacturonan II synthesized by the L-fucose-deficient *mur1 Arabidopsis* mutant. *Planta* **219**, 147–157.
- Ridley, B.L., O'Neill, M.A., and Mohnen, D. (2001). Pectins: Structure, biosynthesis, and oligogalacturonide-related signaling. *Phytochemistry* **57**, 929–967.
- Ritzenthaler, C., Nebenführ, A., Movafeghi, A., Stussi-Garaud, C., Behnia, L., Pimpt, P., Staehelin, L.A., and Robison, D.G. (2002). Reevaluation of the effects of Brefeldin A on plant cells using tobacco bright yellow 2 cells expressing Golgi-targeted green fluorescent protein and COPI antisera. *Plant Cell* **14**, 237–261.
- Rodríguez-Carvajal, M.A., Hervé du Penhoat, C., Nazeau, K., Doco, T., and Pérez, S. (2003). The three-dimensional structure of the mega-oligosaccharide rhamnogalacturonan II monomer: A combined molecular modeling and NMR investigation. *Carbohydr. Res.* **338**, 651–671.
- Ruzin, S.E. (1999). *Plant Microtechnique and Microscopy*. (New York: Oxford University Press).
- Ryden, P., Sugimoto-Shirasu, K., Smith, C.S., Findlay, K., Reiter, W.-D., and McCann, M.C. (2003). Tensile properties of *Arabidopsis* cell walls depend on both a xyloglucan cross-linked microfibrillar network and rhamnogalacturonan II-borate complexes. *Plant Physiol.* **132**, 1033–1040.
- Sarria, R., Wagner, T.A., O'Neill, M.A., Faik, A., Wilkerson, C.G., Keegstra, K., and Raikhel, N.V. (2001). Characterization of a family of *Arabidopsis* genes related to xyloglucan fucosyltransferase1. *Plant Physiol.* **127**, 1595–1606.
- Staehelin, L.A., and Driouch, A. (1997). Brefeldin A effects in plants: Are different Golgi responses caused by different sites of action? *Plant Physiol.* **114**, 401–403.
- Staehelin, L.A., and Moore, I. (1995). The plant Golgi apparatus: Structure, functional organization and trafficking mechanisms. *Annu. Rev. Plant Physiol. Plant Mol. Biol.* **46**, 261–288.
- Sterling, J.D., Atmodjo, M.A., Inwood, S.E., Kolli, V.S.K., Quigley, H.F., Hahn, M.G., and Mohnen, D. (2006). Functional identification of an *Arabidopsis* pectin biosynthetic homogalacturonan galacturonosyltransferase. *Proc. Natl. Acad. Sci. USA* **103**, 5236–5241.
- Sterling, J.D., Quigley, H.F., Orellana, A., and Mohnen, D. (2001). The catalytic site of the pectin biosynthetic enzyme α -1,4-galacturonosyltransferase is located in the lumen of the Golgi. *Plant Physiol.* **127**, 360–371.
- Ulvskov, P., Wium, H., Bruce, D., Jørgensen, B., Bruun Qvist, K., Skjøl, M., Hepworth, D.M., Borkhardt, B., and Sørensen, S. (2005). Biophysical consequences of remodeling the neutral side chains of rhamnogalacturonan I in tubers of transgenic potatoes. *Planta* **220**, 609–620.
- Vidal, S., Doco, T., Williams, P., Pellerin, P., York, W.S., O'Neill, M.A., Glushka, J., Darvill, A.G., and Albersheim, P. (2000). Structural characterization of the pectic polysaccharide rhamnogalacturonan II: Evidence for the backbone location of the aceric acid-containing oligoglycosyl side chain. *Carbohydr. Res.* **326**, 277–294.
- Wandall, H.H., Pedersen, J.W., Park, C., Lavery, S.B., Pizette, S., Cohen, S.M., Schwientek, T., and Clausen, H. (2003). *Drosophila* egghead encodes a beta 1,4-mannosyltransferase predicted to form the immediate precursor glycosphingolipid substrate for brainiac. *J. Biol. Chem.* **278**, 1411–1414.
- Willats, W.G.T., McCartney, L., Mackie, W., and Knox, J.P. (2001). Pectin: Cell biology and prospects for functional analysis. *Plant Mol. Biol.* **47**, 9–27.
- York, W.S., Darvill, A.G., McNeil, M., Stevenson, T.T., and Albersheim, P. (1985). Isolation and characterization of plant cell walls and cell wall constitutions. *Methods Enzymol.* **118**, 3–40.
- Zykwińska, A.W., Ralet, M.-C.J., Garnier, C.D., and Thibault, J.-F.J. (2005). Evidence for in vitro binding of pectin side chains to cellulose. *Plant Physiol.* **139**, 397–407.